Time Lapse Seismic Feasibility Study in Carbonate Reservoirs

Ingrid Gomes Guimarães IAG/USP, Liliana Alcazar Diogo IAG/USP

This paper was prepared for presentation during the 13th International Congress of the Brazilian Geophysical Society held in Rio de Janeiro, Brazil, August 26-29, 2013.

Abstract

This paper presents a feasibility seismic time-lapse study applied in Carbonate Reservoirs. We investigate the effects of different saturations of oil and brine in reservoirs composed by calcite and dolomite with vertical fractures (horizontal transversal isotropic medium - HTI) to analyze the enough changes to be detected in a 4D monitoring. The initial studied scenario is the full saturation of oil and the last one is 100% brine saturation. Some reservoir parameters like porosity and composition were varied for studying different types of reservoirs.

Introduction

The importance of Carbonate Reservoirs in the economic scenario of the oil industry is clear: Approximately half of the word's oil and gas reserves are at in this type of reservoir. Their porosity and permeability are lower if we compare with the clastics reservoir, but the high produce is feasible due to fractures, which cause elastic anisotropy in the medium.

Time-lapse or 4D seismic data has proven value in reservoir management, increasing reserves and recovery by locating by passed and undrained hydrocarbons and optimizing infill well locations and flood patterns. 4D seismic can also decrease operating costs by reducing uncertainty in the reservoir geologic model and flow simulation, optimizing completions, and minimizing the number of dry holes.

Feasibility study is the name given to modeling the seismic changes due to predicted production scenarios and determining whether and how reservoir changes can be observed from time-lapse seismic data. If we can predict how rock properties will change, we can predict how the seismic response will change (Rodney Calvert, 2005).

According to Cardona (2002), knowledge of the correct theory for fluid substitution in anisotropic rocks is important for monitoring fluid migration in fracture rocks. When the rock is fluid-saturated, predictions from different theories vary depending on the assumptions made about the pore space connectivity, fluid viscosity and the frequency of the applied stress. Thomsen (1995) studied how the anisotropic parameters of a porous rock with aligned cracks vary with changes in bulk modulus of the saturating fluid. He argues that a correct theory for fluid substitution in fracture sedimentary rocks has to take into account the fluid pressure equilibration that takes place between hydraulically connected cracks and non-fracture pores.

Fluid Substitution Gassmann model (1956) is usually applied in 4D monitoring in the clastic reservoirs. However, in the carbonates this model often produces underestimated velocity changes (Wang et al., 1998; Ander and Brevik, 2000; Tran et al., 2004). A Gassmann generalized theory was adapted to anisotropic rocks, which assumes an isotropic and homogeneous mineral, although the dry rock can present an arbitrary anisotropy. Brown and Korringa (1975) also developed expressions for fluid substitution in anisotropic medium. The result is similar to that obtained by Gassmann, except they assume mineral anisotropy.

In this work we modeled various scenarios representing different carbonate reservoirs with vertical fractures. Porosity, rock composition, and fluid saturation (oil and brine) were varied.

Aiming to correlate the properties of the reservoir with the change of saturation, we analyzed the differences in reflection amplitudes at different times of a simulated production (oil being replaced by brine).

Fluid Substitution Model

Brown and Korringa's theory (1975) is applicable at the low frequency limit, in which pore fluid pressures are allowed to equilibrate. It assumes the rock is 100% fluid saturated and if the rock is stressed, either by a static load or a passing wave, the fluid pressure is equilibrated throughout the pore space. The latter condition can be satisfied in at least three cases: 1) There is a single pore of arbitrary shape in the rock; 2) The rock has a collection of disconnected pores with the same shape and orientation; 3) All pores, with arbitrary shape and orientation, are well connected and the fluid viscosity and frequency of the applied stresses are low enough to allow equilibration of any pressure differences. The third case is one most applicable to fracture sedimentary rocks.

In linear slip model (Bakulin et al., 2000) fractures are treated, regardless of their shape or microstructure, as planes of weakness with non-welded boundary conditions (Schoenberg and Douma, 1988; Schoenberg and Sayers, 1995). When the fractures are embedded in an otherwise isotropic background, the effective compliance matrix (**S**) is given by

$$\mathbf{S} = \mathbf{S}_B + \mathbf{S}_F \quad (1)$$

Where $\mathbf{S}_B$ is the compliance matrix of the isotropic background rock and $\mathbf{S}_F$ is the excess compliance associated with the fractures. The effective compliance of the dry rock ($\mathbf{S}^d$) is given by

$$\mathbf{S}^d = \begin{pmatrix} \frac{1}{E_d}+Z_N^d & -\frac{\nu_d}{E_d} & -\frac{\nu_d}{E_d} & 0 & 0 & 0 \\ -\frac{\nu_d}{E_d} & \frac{1}{E_d} & -\frac{\nu_d}{E_d} & 0 & 0 & 0 \\ -\frac{\nu_d}{E_d} & -\frac{\nu_d}{E_d} & \frac{1}{E_d} & 0 & 0 & 0 \\ 0 & 0 & 0 & \frac{1}{G} & 0 & 0 \\ 0 & 0 & 0 & 0 & \frac{1}{G}+Z_T^d & 0 \\ 0 & 0 & 0 & 0 & 0 & \frac{1}{G}+Z_T^d \end{pmatrix}. \qquad (2)$$

Where Z_N is the excess compliance that relates the fracture-normal displacements to the normal stresses applied to the fracture in the x direction and Z_T is the excess tangential compliance that relates tangential displacements and stresses in the y and z directions, given by:

$$Z_N^d = \frac{16}{3}\frac{1}{E_d}\left(1-\nu_d^2\right)\eta_c,$$

and

$$Z_T^d = \frac{16}{3}\frac{1}{G_d}\left(\frac{1-\nu_d}{2-\nu_d}\right)\eta_c, \qquad (3)$$

where E_d, G_d and ν_d are the Young's modulus, shear modulus and Poisson's ratio of dry background isotropic rock, respectively, and η_c is the crack density.

Brown and Korringa (1975) generalized Gassmann's (1951) work by relaxing the conditions of isotropy and monomineralic rock. In their formulation, Gassmann's scalar equations are replaced by equations that relate the compliance tensor of the dry rock and which can be written as

$$S_{ijkl}^s = S_{ijkl}^d - \frac{\left(S_{ij\alpha\alpha}^d - S_{ij\alpha\alpha}^m\right)\left(S_{kl\alpha\alpha}^d - S_{kl\alpha\alpha}^m\right)}{(c_d-c_m)+(c_f-c_m)\phi_t}. \qquad (4)$$

where S^d_{ijkl} and S^s_{ijkl} are the compliance of the dry and saturated rock, S^m_{ijkl} is the compliance of the mineral material, $\Phi_t = \Phi_i + \Phi_c$ is the total connected porosity, and c_f, c_m and c_d are the fluid, the mineral and the dry rock compressibilities, respectively.

The change in fluid pressure depends on the total storage capacity of the pore system. The total storage capacity relates the variations in pore volume to variations in fluid pressure and is defined as a product of the total porosity (Φ_t) and the total pore system compressibility (c_t). The induced pressure is inversely proportional to Φ_t c_t, because a rock with large storage capacity can accommodate the fluid displacement by the pore volume change with only a small presure variation. The total storage capacity is the sum of the storage capacities of the isotropic pores and crack pores: $\Phi_t c_t = \Phi_i c_i + \Phi_c c_c$, where

$$\phi_i c_i = \left(\frac{1}{K_d}-\frac{1}{K_m}\right)+\left(\frac{1}{K_f}-\frac{1}{K_m}\right)\phi_i, \qquad (5)$$

and

$$\phi_c c_c = Z_N^d + \left(\frac{1}{K_f}-\frac{1}{K_m}\right)\phi_c, \qquad (6)$$

All the elements of the compliance matrix that change with saturation will depend explicitly on both the crack and isotropic porosity. The expressions for the compliance elements that change with saturation are given by:

$$\begin{aligned} S_{11}^s &= \underbrace{\frac{1}{E_d} - \frac{\frac{1}{9}\left(\frac{\phi_i}{K_{\phi_i}}\right)^2}{\phi_t c_t}}_{\approx\frac{1}{E_s}} + \frac{\left(1-\frac{K_f}{K_m}+\frac{K_f}{3K_{\phi_i}}\frac{\phi_i}{\phi_t}\right)Z_N^d}{\frac{K_f}{\phi_t}(\phi_t c_t)}, \\ S_{12}^s = S_{13}^s &= \underbrace{-\frac{\nu_d}{E_d} - \frac{\frac{1}{9}\left(\frac{\phi_i}{K_{\phi_i}}\right)^2}{\phi_t c_t}}_{\approx-\frac{\nu_s}{E_s}} - \frac{\frac{K_f}{3K_{\phi_i}}\frac{\phi_i}{\phi_t}Z_N^d}{\frac{K_f}{\phi_t}(\phi_t c_t)}, \\ S_{22}^s = S_{33}^s &= \frac{1}{E_d} - \frac{\frac{1}{9}\left(\frac{\phi_i}{K_{\phi_i}}\right)^2}{\phi_t c_t} \approx \frac{1}{E_s}, \\ S_{23}^s &= -\frac{\nu_d}{E_d} - \frac{\frac{1}{9}\left(\frac{\phi_i}{K_{\phi_i}}\right)^2}{\phi_t c_t} \approx -\frac{\nu_s}{E_s}, \end{aligned} \qquad (7)$$

So, the compliance matrix for S saturation rock is give by:

$$\mathbf{S}^s \approx \begin{pmatrix} S_{11}^s & S_{12}^s & S_{12}^s & 0 & 0 & 0 \\ S_{12}^s & \frac{1}{E_s} & -\frac{\nu_s}{E_s} & 0 & 0 & 0 \\ S_{12}^s & -\frac{\nu_s}{E_s} & \frac{1}{E_s} & 0 & 0 & 0 \\ 0 & 0 & 0 & \frac{1}{G} & 0 & 0 \\ 0 & 0 & 0 & 0 & \frac{1}{G}+Z_T^s & 0 \\ 0 & 0 & 0 & 0 & 0 & \frac{1}{G}+Z_T^s \end{pmatrix}, \qquad (8)$$

Feasibility Studies

Most reservoirs with unconsolidated rocks, brine, and high-GOR oil, and depths less than 10 000 ft (~3km) show amplitude changes due to fluid or pressure change during production (David E. Lumley et al., 1997). In this work, no reference value was adopted to amplitude changes detectability, considering it depends on numerous factors like type of reservoir and repeatability of acquisition and processing.

For modeling seismic reflection data we utilized the package program ANRAY 4.72 (Psencik and Gajewski, 2012).

Aiming different types of carbonate reservoirs we choice two basic compositions: a reservoir which is only composed by Calcite ($CaCo_3$) and other one formed by Dolomite ($(Ca,Mg)Co_3$). Because our analysis is only at the top of the reservoir, we did not model the complete reservoir overburden. The rock just above the reservoir is halite. The elastic properties of the halite and the carbonates are at table 1. The properties of the fluid contents are at table 2.

Table 1: Elastic constants and density of the rocks applied in the present study.

	Density (kg/m^3)	Font	K_0 (GPa)	μ_0 (GPa)	Font
Halite	2.16	Simmons (1965)	24.8	14.9	Papadakis (1963)
Calcite	2.71		70.2	29	Mavko et. al (1994)
Dolomite	2.87	Nur and Simmons (1969)	94.9	45	

Table 2: Elastic constants and density of the fluids applied in the present study.

	Density (kg/m^3)	K (Gpa)	μ (Gpa)	Font
Oil	0.715	1.05	0	Rogen, 2002 & Aseefa, 2003
Brine	1.03	2.94	0	

The reservoir porosity was varied from 5% to 25% with 5% interval. In all reservoirs the fractures is vertical and parallel (HTI medium) with density of fractures 0.05. The initial saturations in all of them are 100% Oil, and the final are 100% brine. The intermediate scenarios are transitional between these two situations, with 10% interval. We thus study ten different reservoir models and eleven different saturations for each one resulting 110 models.

Results

Three examples of the modeled seismic data are showed in Figure 1. All of them are the reservoir of calcite, with 15% porosity. The seismograms: (1) on the left are generated for the 100% oil saturation model ; (2) in the middle, for 90%, 50% e 0% oil saturation; and on the rigth (3) are the difference of them ((1) – (2)). The resultsshow the difference growing up as the increasing reservoir brine saturation

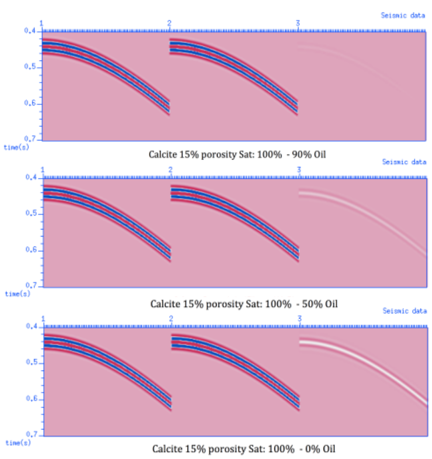

Figure1: Seismograms for calcite reservoir with 15% porosity: on thr left (1) 100% oil saturation; in the midlle (2) the scenarios to 90%, 50% e 0% oil saturation; and on the right (3) the difference of them ((1)-(2)).

The relative percentage amplitude changes (Rpp relative) with respect to the initial stage of 100% oil saturation are presented in Figures 2 and 3, respectively to calcite and dolomite reservoirs with varing porosity. These amplitudes changes are depicted in function of incident angles. Each curve refers to a different saturation scenario. The angles of incidence used in the graph are smaller than the critical angle.

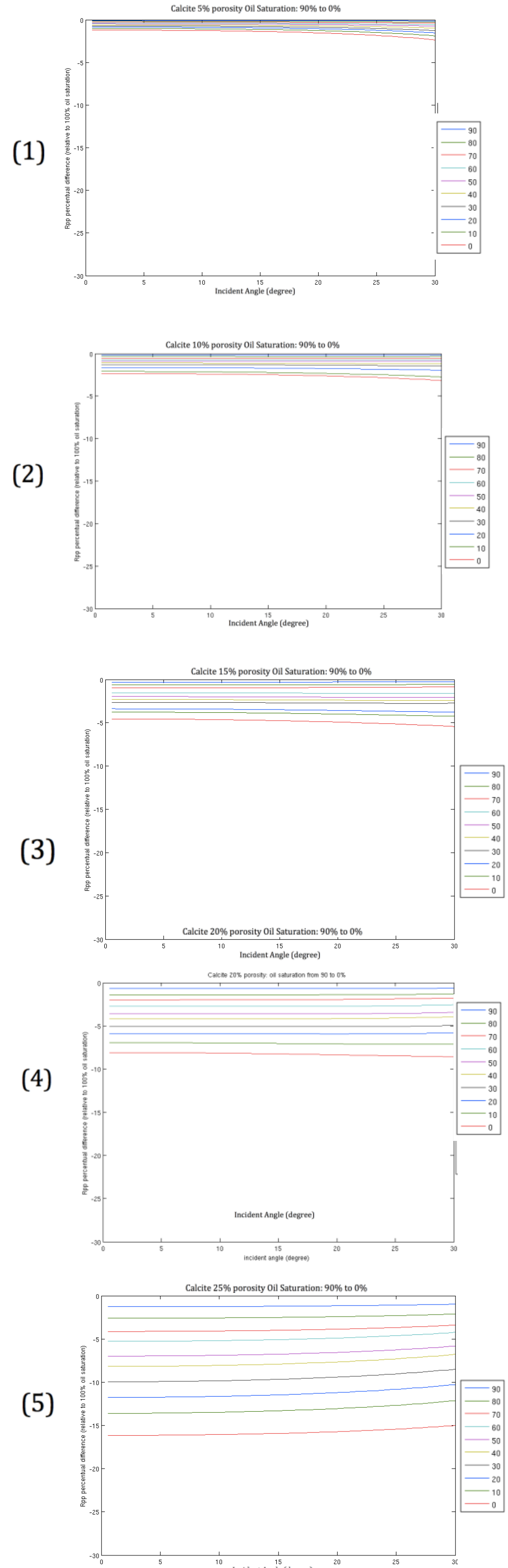

Figure 2: Charts 1-5: Relative percentage amplitude changes in Reflection Amplitude (Rpp) with respect to the initial stage of 100% oil saturation to calcite reservoir rock with porosities of: 5% (1); 10% (2), 15% (3), 20% (4), and 25% (5).

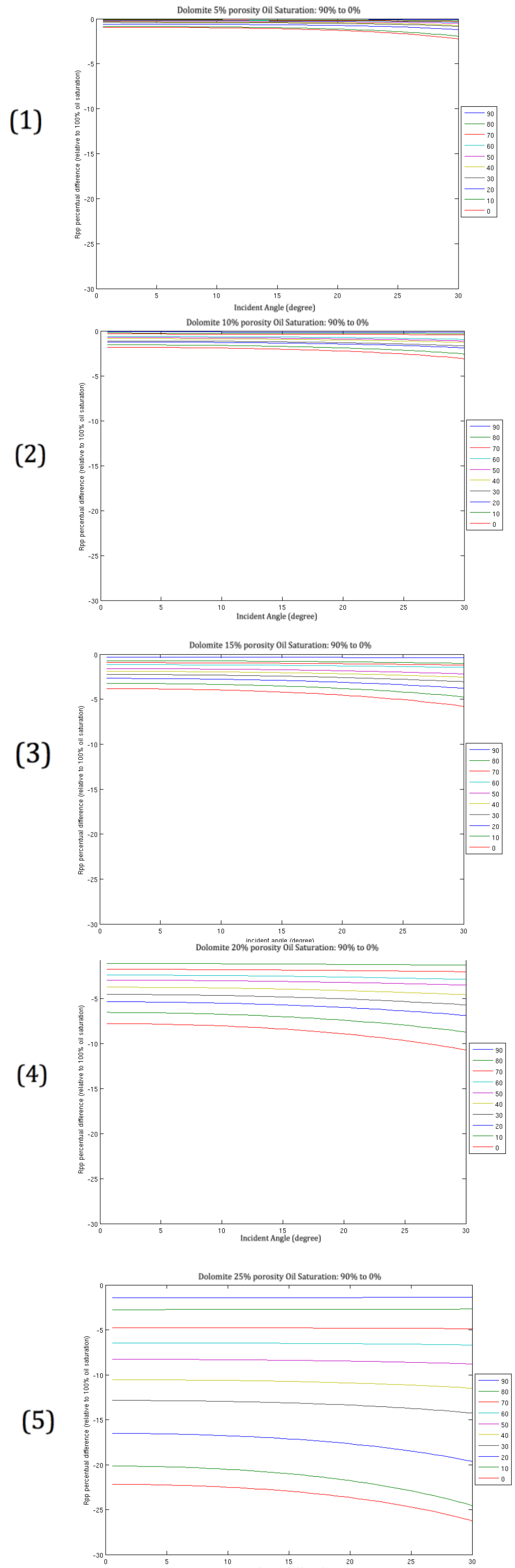

Figure 3: Charts 1-5: Relative percentage amplitude changes in Reflection Amplitude (Rpp) with respect to the initial stage of 100% oil saturation to dolomite reservoir rock with porosities of: 5% (1); 10% (2), 15% (3), 20% (4), 25% (5).

The main observations for both reservoirs are:

i) The greater the porosity of the matrix, the greater is the change in seismic data due to the replacement fluid;

ii) As the brine replaces the oil, the relative amplitude is greater;

iii) The difference of Rpp does not vary with the incident angles for smallest angles;

iv) For fluid substitution greater than 50%, with the exception of 25% porosity calcite reservoir, the greater is the incidente angle, greater is the amplitude differences.

Calcite reservoir

The main observations for calcite reservoir (Figure 2) are:

i) For porosities of 5%, 10% and 15% it is not detected a change in the rock physical parameters able to generate an amplitude change greater than 6%;

ii) For 20% porosity, the relative amplitudes greater than 6% were found only in 20% oil saturation. The maximum value for difference was 9.3%;

iii) For 25% porosity, amplitude changes greater than 6% occurred since 50% oil saturation and greater than 10% in 30% oil saturation. The maximum value for difference was16.2%;

Dolomite reservoir

The main observations for dolomite reservoir (Figure 3) are:

i) For porosities of 5%, 10% and 15% it is not detected a change in the rock physical parameters able to generate an amplitude change greater than 6%;

ii) For 20% porosity, amplitude changes greater 6% were seen in 20% oil saturation. Maximum difference value was 10.5%;

iii) For 25% porosity, amplitude changes greater than 6% existed since 60% oil saturation, greater than 10% in 40% oil saturation and greater than 20% in 20% oil saturation. Maximum difference value was 26%.

Conclusions

Seismic data were modeled with different porosities and oil saturations for two rock compositions, calcite and dolomite, to study the feasibility of applying 4D seismic in carbonate reservoirs to oil replacement. For a given porosity, the saturation was varied from 100% oil until all the fluid was replaced by brine. Were plotted graphs for 5 different porosities, relating the oil saturation to amplitude changes in function of incident angle.

For both reservoirs amplitudes changes greater than 6% were only possible for 20% porosity after oil decreases to 20% saturation. In general, changes greater than 10% occurred only for 25% porosity, in 50% oil saturation for calcite reservoir and 40% oil saturation for dolomite reservoir.

The seismic 4D signal was stronger for dolomite reservoir.

References

Anders, R. S., and I. Brevik, 2000, Fluid substitution in carbonate rocks: Scattering vs. Gassmann theory: 70th Annual International Meeting, SEG, Expanded Abstracts, 1907–1910.

Assefa, S., C. McCann, and J. Sothcott, 2003, Velocities of compressional and shear waves in limestones: Geophysical Prospecting, **51**, 1–13.

Bakulin, A., Grechka, V., and Tsvankin, I., 2000, Estimation of fracture parameters from reflection seismic data - part I: HTI model due to a single fracture set: Geophysics 65, 1788-1802

Brown, J., and Korringa, J., 1975, On the dependence of the elastic properties of a porous rock on the compressibility of the pore fluid: Geophysics 40, 608-616.

Calvert, R., 2005. Insights and method for 4D reservoir monitoring ad characterization. Distinguished Instructor Short Course, SEG and EAGE, n8.

Cardona, R., 2002, Topics on the Seismic Charactheriation of Fractures Reservoirs,Ph.D Thesis, Colorado School of Mines.

GASSMANN, F., 1951. Uber die Elastizitat poroser Medien, Vierteljahrsschrift der Naturforschenden Gesellschaft in Zurich, 96, 1-23.

Mukerji, T. and Mavko, G., 1994. Pore fluid effects on seismic velocity in anisotropic rocks, Geophysics, 59, 233-244

Nur, A. and Simmons, G., 1969a. Stress-induced velocity anisotropy in rocks: an experimental study. J. Geophys. Res., 74, 6667.

Papadakis, E.P., 1963. Attenuation of pure elastic modes in NaCl single crystals. J. Appl. Phys.,34, 1872–1876.

Psencik, I. and Gajewski, D., Package Program ANRAY:http://seis.karlov.mff.cuni.cz/software/sw3dcd16/anray/anray.htm

Rogen, B., 2002, North Sea Chalk-textual and petrophysical properties: Ph.D. thesis, Environment and Resources DTU, Technical University of Denmark.

Simmons, G., 1965. Single crystal elastic constants and calculated aggregate properties. J. Grad.Res. Center, SMU, 34, 1–269.

Thomsen, L., 1995, Elastic Anisotropy due to aligned cracks on porous rock: Elastic anisotropic due to aligned cracks on porous rock, Eur. Assn. Geosci. Eng., Geophy. Prosp.

Tran, H., L. R. Bently, and E. S. Krebes, 2004, Use of time-lapse analysis to predict fluid changes in carbonate pool: A case study of the Rainbow B pool: CSEG, Expanded Abstracts, 057S011, 1–4.

Wang, Z., M. E. Cates, and R. T. Langan, 1998, Seismic monitoring of a CO2 flood in carbonate reservoir: A rock physics study: Geophysics, 63, 1604–1617.